Efficiency enhancement of polymer solar cells by post-additional annealing treatment*

YU Xuan (余璇), **YU Xiao-ming** (于晓明), **HU Zi-yang** (胡子阳), **ZHANG Jian-jun** (张建军)**, **ZHAO Geng-shen** (赵庚申), **and ZHAO Ying** (赵颖)

Key Laboratory of Photo-electronic Thin Film Devices and Technology of Tianjin, Key Laboratory of Opto-electronic Information Science and Technology for Ministry of Education, Institute of Photo-electronic Thin Film Devices and Technology, Nankai University, Tianjin 300071, China

(Received 12 March 2013)

We adopt the post-additional thermal annealing (PATA) process to optimize the performance of the polymer solar cells (PSCs) with an active layer composed of a blend of regioregular poly (3-hexythiophene) (RR-P3HT) and fullerenes. It is found that compared with general annealing process, the crystallinity of RR-P3HT by PATA is enhanced, and the absorption peak is raised obviously at ~500 nm after PATA. With the optimized annealing conditions, the device shows an enhancement of 31% in short circuit current density, 5% in open circuit voltage (V_{oc}), and 11% in the power conversion efficiency (PCE) compared with that of the general annealing device.

Document code: A **Article ID:** 1673-1905(2013)04-0274-4

DOI 10.1007/s11801-013-3044-0

Polymer solar cells (PSCs) have attracted lots of attention due to their light weight, low manufacture cost, potential of large-scale fabrication and fast progress in power conversion efficiency (PCE) since the discovery of efficient electron transfer between conjugated polymers and fullerenes in bulk heterojunction (BHJ) PSCs[1-3]. At present, BHJ PSCs have exhibited the PCE above 8% by using new donor-acceptor material and designing novel device structure[1,4]. Among many candidate materials, the BHJ system consisting of regioregular (RR) poly (3-hexythiophene) (P3HT) and [6, 6]-phenyl C_{61} butyric acid methyl ester (PCBM) has been extensively researched[5,6], for its excellent features of charge transportation and light-harvesting. Furthermore, the performance of PSCs can be largely improved just by simple annealing process with outstanding interpenetrating nanoscale networks[7].

Since 2002, systematic researches on the principle and way of annealing treatment[8-14] have been made, such as annealing temperature and time[15-17] of post-production thermal annealing (TA), organic solvent with different solubilities[11] and the ratio of donor-accepter blend[9] of solvent annealing (SA) process. It is well known that the improved morphology with nanoscale interpenetrating network could enhance the efficiency of devices after the TA treatment. However, Jang Jo et al[10] found that the fast diffusion and aggregation of PCBM would have bad impact on the P3HT crystallization during high temperature TA. Also, there are various factors to be considered in the annealing process, for instance air humidity, room temperature[18], etc. Until now, the best annealing condition for P3HT:PCBM system is still controversial. Moreover, the optimization in interpenetrating network and surface morphology is significant for improving PSCs' performance. Thereby, in this paper, we conduct the post-additional thermal annealing (PATA) treatment in order to further investigate the ordered morphology between the crystallization of P3HT and the growth of PCBM. The results of experiment demonstrate that the PATA process is more effective for enhancing the performance of PSCs compared with other TA methods.

The indium tin oxide (ITO) glass substrates were strictly cleaned with detergent, and then rinsed in an ultrasonic bath in acetone, ethanol, deionized water for 15 min each. These substrates were baked in an oven at 80 °C for 3 h. RR-P3HT:PCBM mixture with a weight ratio of 1:0.8 containing 10 mg·mL^{-1} P3HT and 8 mg·mL^{-1} PCBM in chlorobenzene was stirred at 30 °C overnight. A thin layer (~40 nm) of PEDOT:PSS (CLEVIOS P VP AI 4083) was spin-coated onto the cleaned ITO substrates with a speed of 2000 r/min for 40 s to form the hole- transport layer. The films were then baked at 135 °C for 30 min. The RR-P3HT:PCBM blend was subsequently spin-coated on the PEDOT:PSS layer with a speed of 400 r/min for 12 s. Finally, 1 nm-thick LiF and 100 nm-thick Al films were thermally deposited under

* This work has been supported by the National Basic Research Program of China (Nos.2011CBA00705, 2011CBA00706 and 2011CBA00707), and the Major Science and Technology Support Project of Tianjin (No.11TXSYGX22100).

** E-mail: jjzhang@nankai.edu.cn

10^{-4} Pa as the cathode. The schematic diagram of the device structure is shown in Fig.1.

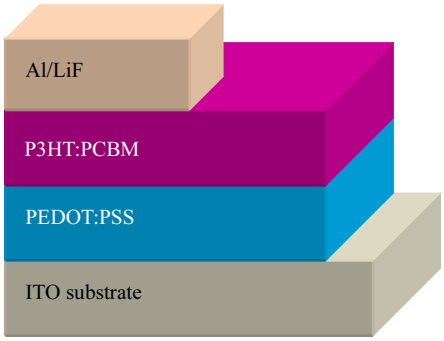

Fig.1 Schematic diagram of the proposed PSCs' structure

SA was carried out by directly putting the substrates with spin-coated active layer into covered petri dishes for 4 h at room temperature. In TA process, the production devices were placed on a hot plate at 110 °C for 5 min. Post-additional thermal annealing (PATA) treatment is as follows: the samples coated with active layer were through SA for 4 h firstly, cathode is thermally evaporated for the preparation of the integrated devices, and then the thermal process is conducted.

Surface roughness and morphology of thin films were characterized by atomic force microscopy (AFM) on a Seiko SPA-400. X-ray diffraction (XRD) patterns of the P3HT:PCBM films were measured by a Rigaku X-ray diffractometer (D/max-2500). Optical transmission spectra were recorded using a Cary spectrophotometer. The current density-voltage (*J-V*) characteristics were measured with a Keithley 4200 sourcemeter under AM 1.5G (100 mW/cm^2) solar simulator. The fabrication and characterization of device were performed in ambient condition in air.

It is very important to control the morphology of the bulk-heterojunction (BHJ) for improving the performance of PSCs, due to the separation of excitons is increased at the interface between the donor and accepter[19]. From the AFM images, it is clear to observe that the active layer presents an obscure surface without any annealing process as shown in Fig.2(a), so it is hard to distinguish the two components as the interpenetrating network is not well developed yet[9]. As shown in Fig.2(b), the distinct phase-separation appears due to the enough time for self-organization of RR-P3HT after SA for 4 h, so the network is gradually formed. The morphologies of active layer after TA and PATA treatments are shown in Fig.2(c) and (d), respectively. After the TA process at 110 °C for 5 min, the interpenetrating networks become easily visible. The surface of active layer conducted by PATA process shows a clearer donor-accepter domain, and the root-mean-square (RMS) of active layer is increased from 0.83 nm to 1.26 nm, simultaneously.

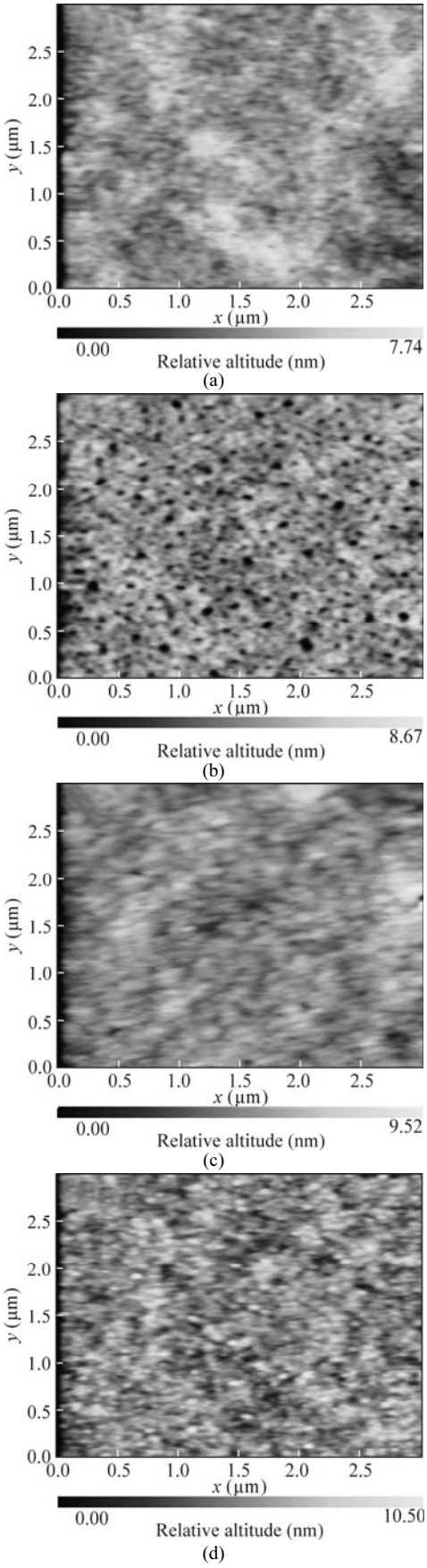

Fig.2 AFM images of the surfaces of active layers (a) before and after (b) SA, (c) TA and (d) PATA treatments, respectively

The annealing treatment has an important impact on the crystallinity of P3HT. We can observe the increased crystallinity of RR-P3HT in XRD results as shown in Fig.3. Compared with TA treatment, the crystallinity is increased in the peak at 2θ=5° after PATA process. Due to in the PATA method based on SA procedure, the conjugated chain is fully self-assembled to be orderly structure, the length of conjugated bond is increased, and the growth and diffusion of PCBM are accelerated in the TA process, a developed interpenetrating network morphology is formed, which improves the crystallinity of RR-P3HT and facilitates the charge transport to the electrodes[9].

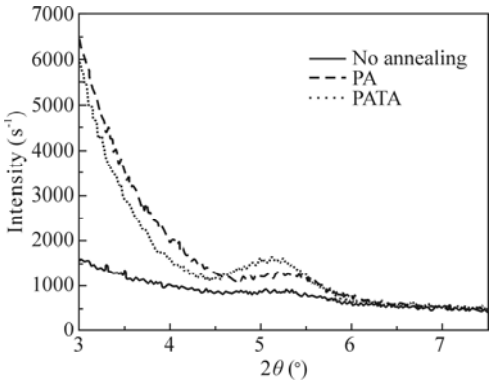

Fig.3 XRD patterns of P3HT:PCBM blend films based on different annealing processes

Effects of the two annealing treatments on the ultraviolet-visible (UV-vis) absorption spectra of RR-P3HT: PCBM blend films with weight ratio of 1:0.8 are shown in Fig.4. Compared with no annealing treatment, there is an apparent red-shift of the absorption spectrum in the wavelength from 498 nm to 600 nm of P3HT after TA methods, which is attributed to an increased chain interaction among P3HT chains. However, UV-vis absorption of P3HT film after TA is insufficient due to the film grows too fast and the orientation of P3HT is forced during the TA process[10], compared with the film after PATA process. Because of the enough time for self-organization, the super-molecules of P3HT can achieve a stable state of thermodynamics during SA[7], and it results in the enhanced absorption from 450 nm to 550 nm for the film after PATA process, which also represents a higher crystallinity of RR-P3HT and is consistent with the result of XRD studies.

The *J-V* characteristics of PSCs based on different annealing processes are shown in Fig.5(a), and the short current density (J_{sc}), the open circuit voltage (V_{oc}), the fill factor (*FF*) and the PCE of the devices before and after two annealing processes are listed in Tab.1. One hand, the increased RMS of BHJ increases the contact area at the interface between active layer and cathode, facilitates the Al diffusion or chemical reactions, and gets a better interfacial adhesion[20]. The other hand, the rough electrode can trap light effectively[21], thus increasing

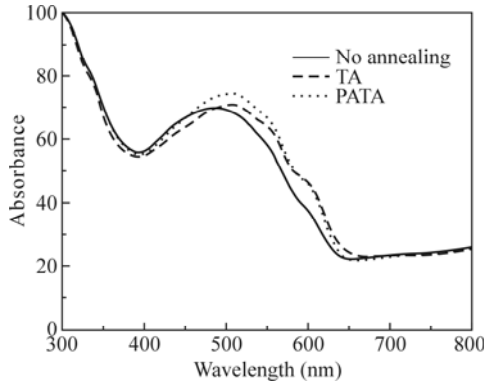

Fig.4 UV-vis absorption spectra for P3HT:PCBM films based on different annealing processes

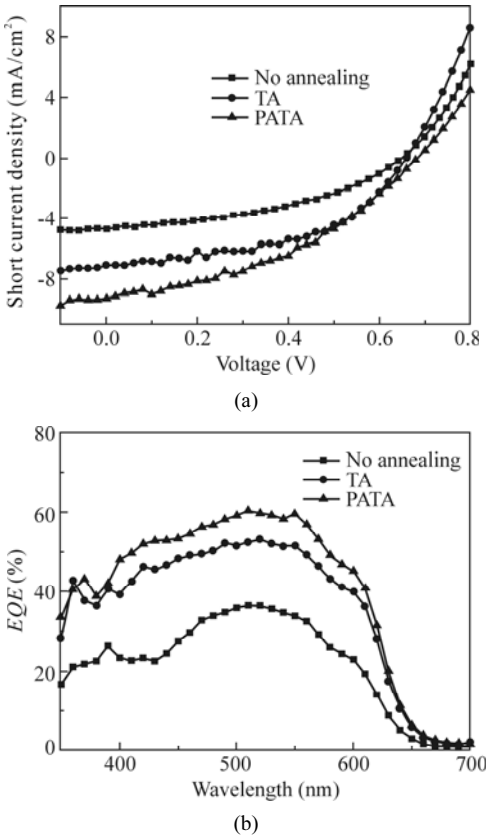

Fig.5 (a) *J-V* characteristics under AM 1.5G simulated illumination and (b) *EQE* of devices

light absorption. TA treatment at 110 °C for 5 min improves the interface between the cathode and active layer, and the nanoscale phase separation results in the improvement of PCE from 1.26% to 2.34%. During SA process, P3HT is fully self-assembled along with the evaporation of organic solution, which increases the order of structure and hole mobility[11]. However, there might still be residual solvent in active layer because of the high boiling point of chlorobenzene (132.2 °C) through the long time slow growth at room temperature, so the orientation of molecule can not reach the stable thermo-

dynamic state. We conduct PATA process, during which the solvent is able to evaporate entirely, and at the same time PCBM is prevented from overgrowing effectively, which can give rise to obstruct the crystallization of P3HT and reduce the length of conjugated chain[22] during the self-assembly of RR-P3HT. Therefore, J_{sc} of the device after PATA process is greatly enhanced from 7.1 mA/cm^2 to 9.27 mA/cm^2, the external quantum efficiency (*EQE*) of the PATA device is also increased as shown in Fig.5(b), and V_{oc} from 0.62 V to 0.65 V results in much-improved device PCE of 2.59%.

Tab.1 Detailed performance parameters of the PSCs

Sample	J_{sc} (mA/cm^2)	V_{oc} (V)	*FF*	*PCE* (%)	Annealing
1	4.72	0.59	0.45	1.26	No annealing
2	7.10	0.62	0.53	2.34	TA: 110 °C, 5 min
3	9.27	0.65	0.42	2.59	PATA: SA(4 h)+ TA(110 °C, 5 min)

We investigate the effect of the PATA treatment on the performance of PSCs. The results indicate that the crystallization and the surface roughness of RR-P3HT are both improved after PATA compared with those after TA treatment. The better interpenetrating network formed between RR-P3HT and PCBM is convenient for charge transfer and extraction, therefore the PCE of PATA device is improved by about 11%. Our results suggest that PATA treatment is an easy and feasible way to conduct, and will be of great importance in large-scale fabrication of PSCs.

References

[1] He Z., Zhong C., Huang X., Wong W.-Y., Wu H., Chen L., Su S. and Cao Y., Adv. Mater. **23**, 4636 (2011).

[2] Zhou H., Yang L. and You W., Macromolecules **45**, 607 (2012).

[3] Yu G., Gao J., Hummelen J. C., Wudl F. and Heeger A. J., Science **270**, 1789 (1995).

[4] Li X., Choy W. C. H., Huo L., Xie F., Sha W. E. I., Ding B., Guo X., Li Y., Hou J., You J. and Yang Y., Adv. Mater. **24**, 3046 (2012).

[5] Li W. M., Guo J. C. and Zhou B., Journal of Optoelectronics·Laser **23**, 1274 (2012). (in Chinese)

[6] Yan Q. Q., Qin W. J., Wang C., Song P. F., Ding G. J., Yang L. Y. and Yin S. G., Optoelectronics Letters **7**, 410 (2011).

[7] Li G., Shrotriya V., Hang J. S., Yao Y., Moriarty T., Emery K. and Yang Y., Nat. Mater. **4**, 864 (2005).

[8] Padinger F., Rittberger R. S. and Sariciftci N. S., Adv. Funct. Mater. **13**, 1 (2003).

[9] Ma W. L., Yang C. Y., Gong X., Lee K. and Heeger A. J., Adv. Funct. Mater. **15**, 1617 (2005).

[10] Jo J., Kim S. S., Na S. I., Yu B. K. and Kim D. Y., Adv. Funct. Mater. **19**, 866 (2009).

[11] Park J. H., Kim J. S., Lee J. H., Lee W. H. and Cho K., J. Phys. Chem. C **113**, 17579 (2009).

[12] Li G., Yao Y., Yang H., Shrotriya V., Yang G. and Yang Y., Adv. Funct. Mater. **17**, 1636 (2007).

[13] Li W. J., Journal of Optoelectronics·Laser **21**, 1602 (2010). (in Chinese)

[14] Zhang Y. P., Journal of Optoelectronics·Laser **20**, 1327 (2009). (in Chinese)

[15] Kim J. Y., Kim S. H., Lee H. Ho, Lee K., Ma W., Gong X. and Heeger A. J., Adv. Mater. **18**, 572 (2006).

[16] Riedel M. and Dyakonov V., Phys. Status Solidi A **201**, 1332 (2004).

[17] Kim Y., Choulis S. A., Nelson J., Bradley D. D. C., Cook S. and Durrant J. R., Appl. Phys. Lett. **86**, 063502 (2005).

[18] Hu Z., Zhang J. and Zhu Y., Appl. Phys. Lett. **102**, 043307 (2013).

[19] Dennler G., Scharber M. C. and Brabec C. J., Adv. Mater. **21**, 1323 (2009).

[20] Lögdlund M. and Brédas J. L., J. Chem. Phys. **101**, 4357 (1994).

[21] Hu Z., Zhang J. and Zhao Y., Org. Electron. **13**, 142 (2012).

[22] Swinnen A., Haeldermans I., Van de Ven M., D'Haen J., Vanhoyland G., Aresu S., D'Olieslaeger M. and Manca J., Adv. Funct. Mater. **16**, 760 (2006).